AALBORG UNIVERSITY

DENMARK

The Inter Facility Testing of a Standard Oscillating Water Column (OWC) Type Wave Energy Converter (WEC)

Andersen, Morten Thøtt; Thomsen, Jonas Bjerg

Citation for published version (APA):
Andersen, M. T., & Thomsen, J. B. (2014). The Inter Facility Testing of a Standard Oscillating Water Column (OWC) Type Wave Energy Converter (WEC). Aalborg: Department of Civil Engineering, Aalborg University. (DCE Technical Reports; No. 180).

MARINET

Marine Renewables Infrastructure Network

Comparative Testing Report

The Inter Facility Testing of a Standard Oscillating Water Column (OWC) Type Wave Energy Converter (WEC).

[The Round Robin Programme]

Facilities:
ECN;
Plymouth University;
HMRC @ UCC;
Edinburgh University;
Aalborg University;
Strathclyde University.

ABOUT MARINET
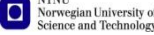
MARINET (Marine Renewables Infrastructure Network for emerging Energy Technologies) is an EC-funded network of research centres and organisations that are working together to accelerate the development of marine renewable energy - wave, tidal & offshore-wind. The initiative is funded through the EC's Seventh Framework Programme (FP7) and runs for four years until 2015. The network of 29 partners with 42 specialist marine research facilities is spread across 11 EU countries and 1 International Cooperation Partner Country (Brazil).

MARINET offers periods of free-of-charge access to test facilities at a range of world-class research centres. Companies and research groups can avail of this Transnational Access (TA) to test devices at any scale in areas such as wave energy, tidal energy, offshore-wind energy and environmental data or to conduct tests on cross-cutting areas such as power take-off systems, grid integration, materials or moorings. In total, over 700 weeks of access is available to an estimated 300 projects and 800 external users, with at least four calls for access applications over the 4-year initiative.

MARINET partners are also working to implement common standards for testing in order to streamline the development process, conducting research to improve testing capabilities across the network, providing training at various facilities in the network in order to enhance personnel expertise and organising industry networking events in order to facilitate partnerships and knowledge exchange.

The aim of the initiative is to streamline the capabilities of test infrastructures in order to enhance their impact and accelerate the commercialisation of marine renewable energy. See www.fp7-marinet.eu for more details.

Partners

Ireland
University College Cork, HMRC (UCC_HMRC)
Coordinator

Sustainable Energy Authority of Ireland (SEAI_OEDU)

Denmark
Aalborg Universitet (AAU)

Danmarks Tekniske Universitet (RISOE)

France
Ecole Centrale de Nantes (ECN)

Institut Français de Recherche Pour l'Exploitation de la Mer (IFREMER)

United Kingdom
National Renewable Energy Centre Ltd. (NAREC)

The University of Exeter (UNEXE)

European Marine Energy Centre Ltd. (EMEC)

University of Strathclyde (UNI_STRATH)

The University of Edinburgh (UEDIN)

Queen's University Belfast (QUB)

Plymouth University(PU)

Spain
Ente Vasco de la Energía (EVE)

Tecnalia Research & Innovation Foundation (TECNALIA)

Belgium
1-Tech (1_TECH)

Netherlands
Stichting Tidal Testing Centre (TTC)

Stichting Energieonderzoek Centrum Nederland (ECNeth)

Germany
Fraunhofer-Gesellschaft Zur Foerderung Der Angewandten Forschung E.V (Fh_IWES)

Gottfried Wilhelm Leibniz Universität Hannover (LUH)

Universitaet Stuttgart (USTUTT)

Portugal
Wave Energy Centre – Centro de Energia das Ondas (WavEC)

Italy
Università degli Studi di Firenze (UNIFI-CRIACIV)

Università degli Studi di Firenze (UNIFI-PIN)

Università degli Studi della Tuscia (UNI_TUS)

Consiglio Nazionale delle Ricerche (CNR-INSEAN)

Brazil
Instituto de Pesquisas Tecnológicas do Estado de São Paulo S.A. (IPT)

Norway
Sintef Energi AS (SINTEF)

Norges Teknisk-Naturvitenskapelige Universitet (NTNU)

The Inter Facility Testing of a Standard Oscillating Water Column (OWC) Type Wave Energy Converter (WEC)

Morten Thøtt Andersen
Jonas Bjerg Thomsen

DEPARTMENT OF CIVIL ENGINEERING
AALBORG UNIVERSITY

Aalborg University
Department of Civil Engineering
Wave Energy Research Group

DCE Technical Report No. 180

The Inter Facility Testing of a Standard Oscillating Water Column (OWC) Type Wave Energy Converter (WEC)

by

Morten Thøtt Andersen
Jonas Bjerg Thomsen

December 2014

Scientific Publications at the Department of Civil Engineering

Technical Reports are published for timely dissemination of research results and scientific work carried out at the Department of Civil Engineering (DCE) at Aalborg University. This medium allows publication of more detailed explanations and results than typically allowed in scientific journals.

Technical Memoranda are produced to enable the preliminary dissemination of scientific work by the personnel of the DCE where such release is deemed to be appropriate. Documents of this kind may be incomplete or temporary versions of papers· or part of continuing work. This should be kept in mind when references are given to publications of this kind.

Contract Reports are produced to report scientific work carried out under contract. Publications of this kind contain confidential matter and are reserved for the sponsors and the DCE. Therefore, Contract Reports are generally not available for public circulation.

Lecture Notes contain material produced by the lecturers at the DCE for educational purposes. This may be scientific notes, lecture books, example problems or manuals for laboratory work, or computer programs developed at the DCE.

Theses are monograms or collections of papers published to report the scientific work carried out at the DCE to obtain a degree as either PhD or Doctor of Technology. The thesis is publicly available after the defence of the degree.

Latest News is published to enable rapid communication of information about scientific work carried out at the DCE. This includes the status of research projects, developments in the laboratories, information about collaborative work and recent research results.

Preface

This report describes the behavior and preliminary performance of a simplified standard oscillating water column (OWC) wave energy converter (WEC). The same tests will be conducted at different scales at 6 different test facilities and the results obtained will be used for comparison. This project will be refereed to as The Round Robin Programme. The rationale for the work is based on the MaRINET proposal:

> A key aspect of the standardisation of device testing is that results from independent trials will be compatible between different test centres. Even when similar procedures are followed this may not be guaranteed. A specially selected test programme will, therefore, be implemented at certain MaRINET facilities to investigate this matter. Due to budget restrictions only laboratory scale centres can be considered but the open water operators will be consulted continuously during the formalisation of the programme to ensure scale similitude of the plan as well as the procedures. The expectation would then be that when the successful devices reach prototype size trials the previous stage results will be compatible.

The experiments have been conducted in the Hydraulics and Coastal Engineering Laboratory at Aalborg University, Sohngaardsholmsvej 57, DK-9000 Aalborg. For further information regarding the content of this report please contact Morten Thøtt Andersen (mta@civil.aau.dk) or Jonas Bjerg Thomsen (jbt@civil.aau.dk) from the Department of Civil Engineering.

<div align="right">Aalborg University, December 12, 2014</div>

Contents

1 | Introduction

The following tests are based on standard operation procedures at the Hydraulics and Coastal Engineering Laboratory at Aalborg University. It should however be noted that when working in the laboratory each project will always be treated individually in both setup and execution.

1.1 Concept

The Round Robin WEC (wave energy converter) is a FOWC-type (floating oscillating water column). This concept utilizes the wave elevation to drive a compression/expansion of and internal air chamber, which in turn drives a turbine/generator. The system uses a slack catenary mooring system for station-keeping.

1.2 Modelling

Since the correct scaling of a turbine PTO (power take-off) is not practically achievable, the PTO will instead be modeled by an orifice cap. The absorbed power of the system is then modeled as the product of the flow through the orifice and the relative chamber pressure. This will described in detail in section 2.3. The report presents the construction and verification of the WEC it self as well as the mooring system in chapter 2 and 3.

2 | Model Construction

The OWC WEC model was constructed at Aalborg University, based on the prescribed full scale values. Because of the test facility at AAU it was determined to construct the model in scale 1:70. The construction of the model is described in the following sections.

2.1 Scaling

For scaling of the model Froude's scaling law was used.

$$x_M = \lambda x_F \tag{2.1}$$

Where x is the parameter to be scaled, subscript M indicates model scale and subscript F indicates full scale. The multiplication factor λ is seen in Table 2.1.

Parameter	Multiplication factor λ
Length [m]	$\lambda_L = L_M / L_F$
Time [s]	$\lambda_T = \lambda_L^{0.5}$
Mass [kg]	$\lambda_m = \lambda_L^3$
Force [N]	$\lambda_f = \lambda_L^3$
Effect [W]	$\lambda_E = \lambda_L^{3.5}$

Table 2.1: Multiplication factors used in Froude scaling of relevant parameters.

2.2 Model description

Using the scaling law, the 1:70 model was constructed with dimensions shown in figure 2.1. Materials were chosen to provide the smallest deviation between prescribed and constructed parameters. This is shown in Table 2.2.

	Model	Full Scale	Prescribed	Deviation [%]
Mass [kg]	2.35	806050	810333.01	0.53
Center of Gravity [m] (above keel)	0.286	20.02	21.14	5.28
Plenum int. diameter [m]	0.0743	5.201	5.200	0.02
Float height [m]	0.1893	13.251	13.250	0.01
Orifice diameter [m]	0.0074	0.518	0.520	0.38

Table 2.2: Physical properties and dimensions of constructed model together with deviation from prescribed full scale values. Cf. Figure 2.2 for definitions.
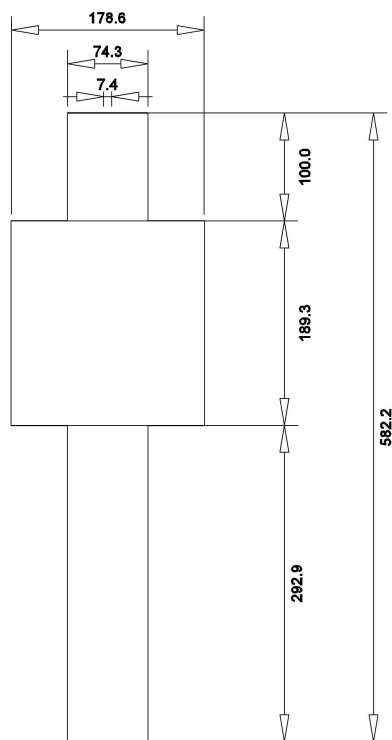
Figure 2.1: Dimensions of constructed model.
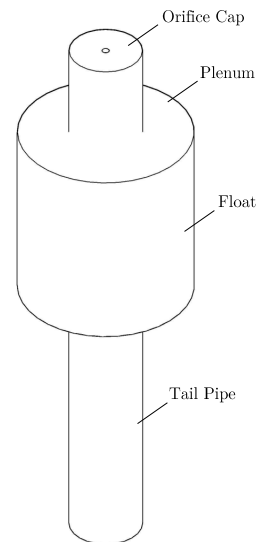
Figure 2.2: Definition of components in model.

The constructed model can be seen in Figure 2.3.
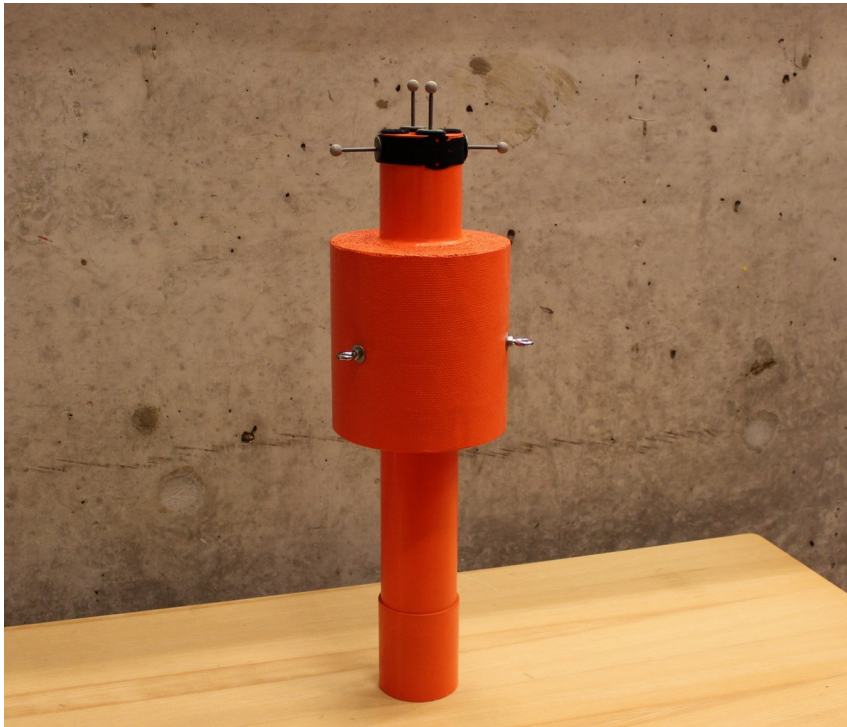
Figure 2.3: Photo of constructed model.

The model was placed in the wave basin in a water depth $h = 0.7$ m. A three-legged catenary mooring system was used in order to keep the model on station. Three bottom anchors were installed and connected to three surface buoys through catenary chains with weight equal to 0.053 kg/m. The surface buoys was connected to the model through three light lines. The mooring system is illustrated in Figure 2.4-2.6.
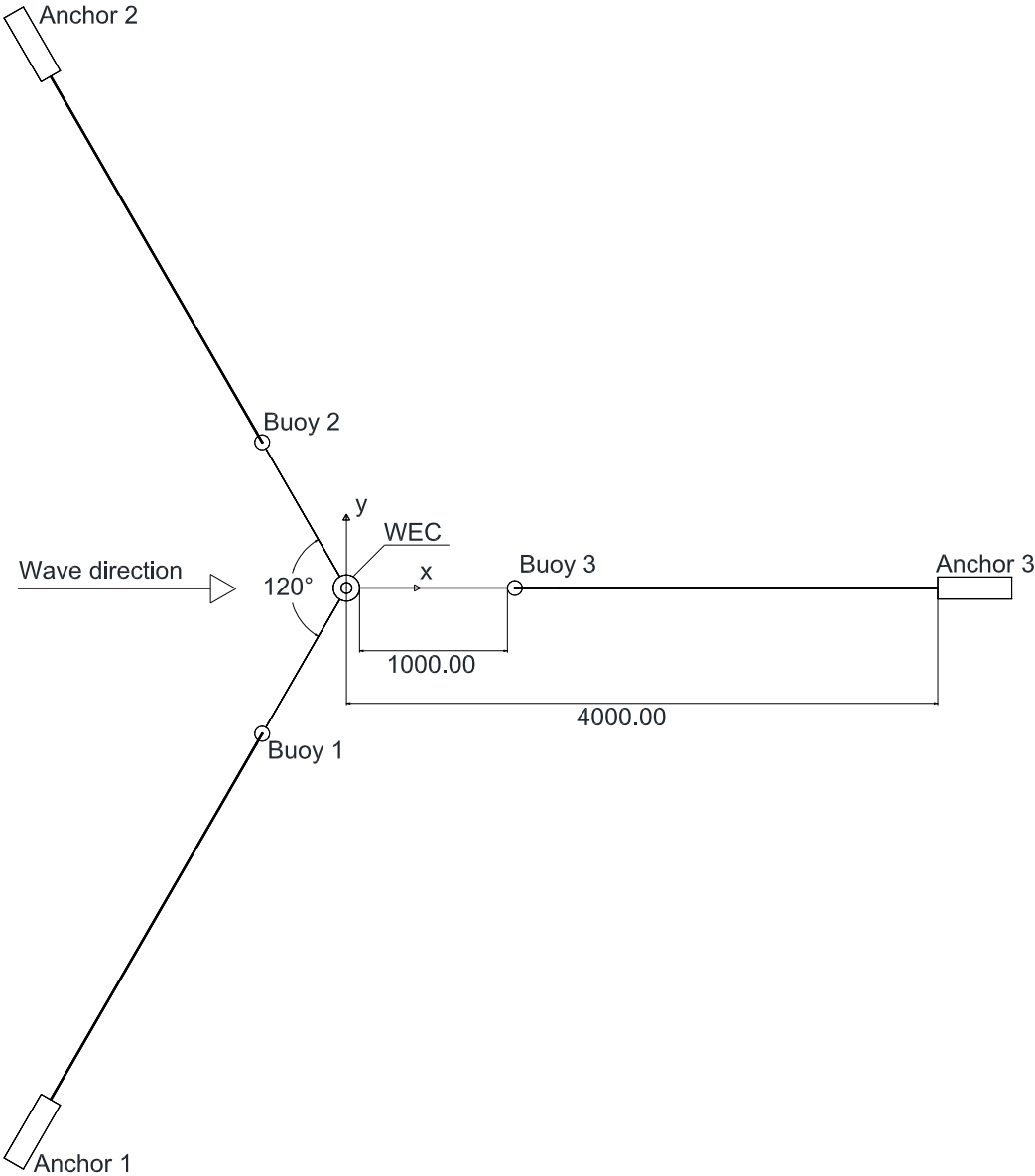
Figure 2.4: Top view of laboratory test set-up. All dimensions are in mm.
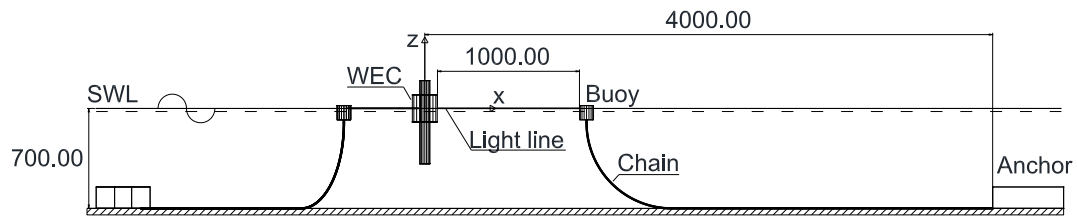
Figure 2.5: Side view of laboratory test set-up. All dimensions are in mm.
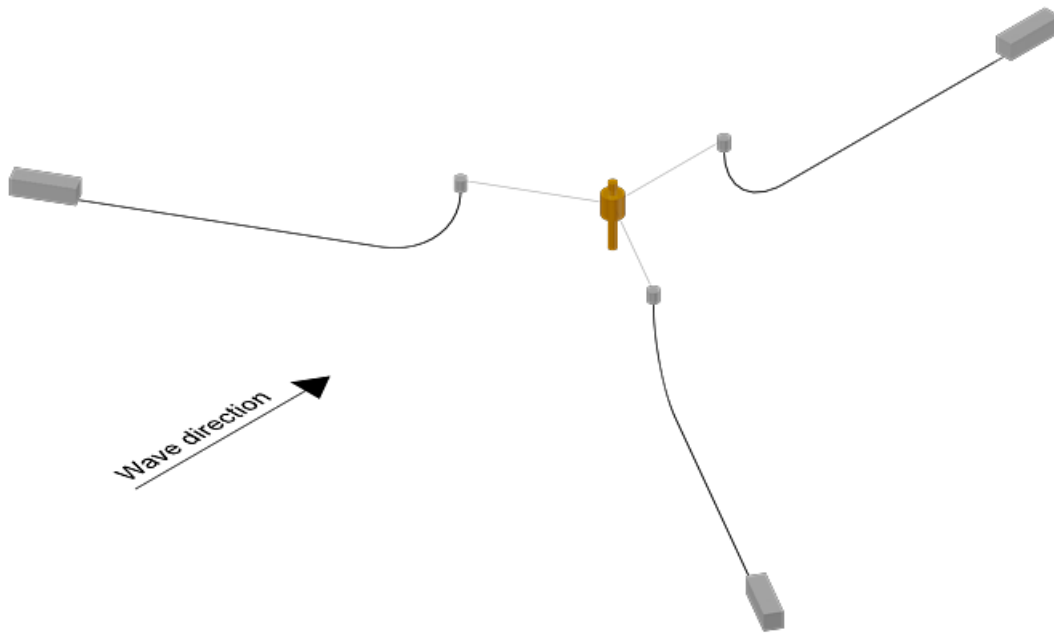

Figure 2.6: 3D model of contructed WEC.

2.3 Sensors

In order to measure incident waves, a total of six resistant type wave gauges were used, located beside the model, cf. Figure 2.7. Acquisition of measured data was done by the software package WaveLab 3 (Andersen and Frigaard [2014]).
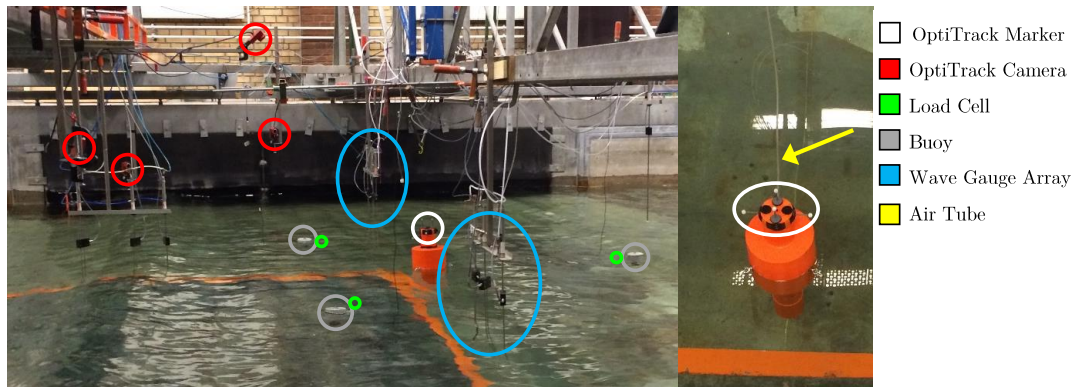
Figure 2.7: Laboratory set-up with used equipment.

To measure the motions of the model during tests, the motion tracking system OptiTrack was used. A total of 4 OptiTrack Flex 13 cameras were installed, together with 5 reflective markers on the model. The software Motive 1.7.1 was used to track the motions. Cf. Figure 2.7 for set-up.

Mooring loads were measured at the connection point between the buoys and the light lines. Load cells of the type FUTEK LSB210 25, 50 and 100 lb was used, cf. Figure 2.8.

For calculation of the absorbed power of the waves, the pressure difference over the orifice relative to the atmospheric pressure was measured, using an installed air tube in the model, as shown in Figure 2.9.
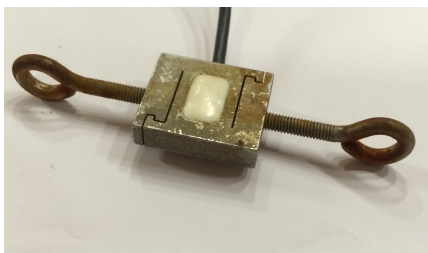
Figure 2.8: Load cell FUTEK LSB210.
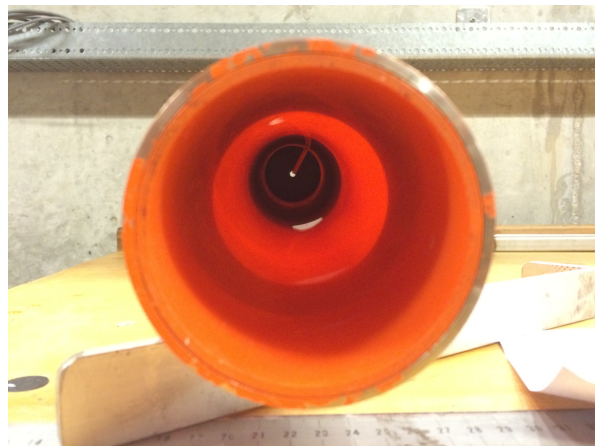
Figure 2.9: Installed air tube in model used for measuring of pressure difference over orifice.

2.4 Power Production

Calculation of the absorbed power is based on equation (2.2).

$$P_{abs}(t) = \Delta P(t)Q(t) = k\left(|\Delta P(t)|\right)^{1.5} \qquad (2.2)$$

$$k = c_d A_d \sqrt{\frac{2}{\rho_{air}}} \qquad (2.3)$$

Where P_{abs} is the absorbed wave power, ΔP is the pressure difference over the orifice, Q is the air flow, t is the time, ρ_{air} is the air density, A_d is the orifice area and c_d is the discharge coefficient. The applied value of c_d is 0.64, which was also determined by previous tests by Nielsen et al. [2013]. For the present test it was attempted to validate this value, but AAU do not have proper equipment for these kind of tests, which resulted in unreliable results. A c_d of 0.64 was therefore used in calculation of the absorbed power. It should be noted that theoretical limits are available for the discharge coefficient. When going from a sharp orifice to a truncated cylinder the c_d raises from 0.62 to 0.88 Joachim [1926]. Since the used orifice is much closer to the sharp case, this applies even more confidence in the applied value of 0.64.

3 | Model Verification

This chapter serves as a verification of the setup explained in chapter 2.

3.1 Motion Response Tests

As seen in appendix B, multiple decay tests are carried out to test if the response of the WEC matches the prescribed behavior. These tests have been conducted on different setups ranging from free-floating body to a fully hooked up system with connected air pressure tube and anchors. This is done to observe the auxiliary systems effect on the response. In the following, only two setups will be presented; the free-floating body, and the fully hooked up system on which all production tests were run. These will be referred to as *body* and *system* respectively.
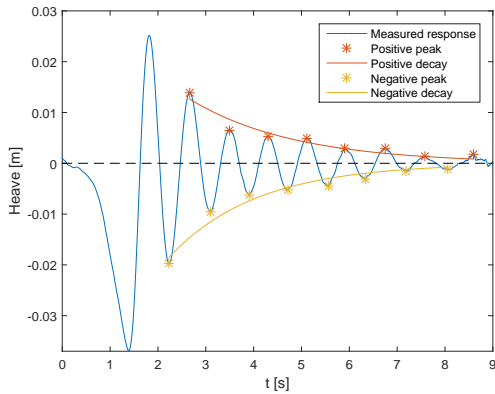
**Figure 3.1:** Heave response of body.
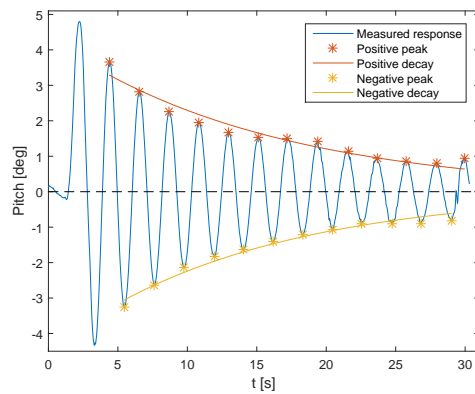
Figure 3.2: Pitch response of body.

3.1.1 Natural Periods

Firstly the eigenperiods of the system is determined from and average distance between the peaks of the decays tests shown in Figure 3.1-3.4. The heave and

11
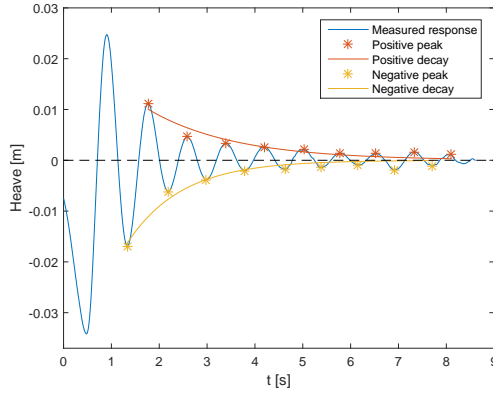
Figure 3.3: Heave response of system.
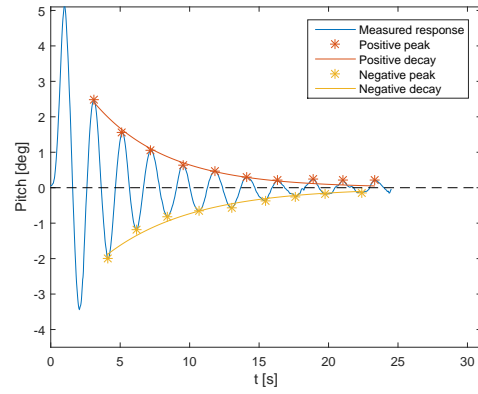
Figure 3.4: Pitch response of system.

pitch period can be seen in Table 3.1. As desired, the heave period of the system matches with the prescribed value. However, it can be seen that the mass distribution is too narrow and hence the 30% lower pitch period. Note: Only the damped periods are shown. The undamped natural periods have been calculated from (3.2), but results vary by less than 0.5% and is therefor neglected in this report.

	Body [s]	System [s]	Full scale [s]	Prescribed [s]	Deviation [-]
Heave	0.86	0.84	6.99	7	1.00
Pitch	2.17	2.06	17.24	25	0.69

Table 3.1: Measured natural periods compared to prescribed values.

3.1.2   Damping

The exponential decay of any single degree of freedom motion can be described from (3.1). Only the decay of the amplitudes are of interest in this report, and hence only the enveloping curve $x = ae^{-\gamma t}$ is calculated.

$$x = ae^{-\gamma t}\cos(\omega_d t - \alpha) \tag{3.1}$$

$$\omega_d = \sqrt{\omega_0^2 - \gamma^2} \tag{3.2}$$

The average of the positive and negative envelope in Figure 3.1-3.4 have been used to describe the given decay. The first two peaks in each run have not been considered in order to remove some of the inevitable nonlinear effects of manually excited single degree of freedom decay tests. In Figure 3.5 the initial

amplitudes have been normalized in order to compare the different responses. The enveloping curve is then described as:

$$\pm x = \pm e^{-\gamma t} \qquad (3.3)$$

The damping coefficient, γ, can be seen in Table 3.2. Here the calm-down time, $t_{0.01}$, is also shown. The calm-down time is a more tangible measure that describes the time at which only 1% of the motion amplitude remains.

	Body		System	
	Heave	Pitch	Heave	Pitch
γ [-]	0.50	0.07	0.72	0.18
$t_{0.01}$ [s]	9.2	69.5	6.4	26.2

Table 3.2: Damping coefficients and corresponding calm-down times.
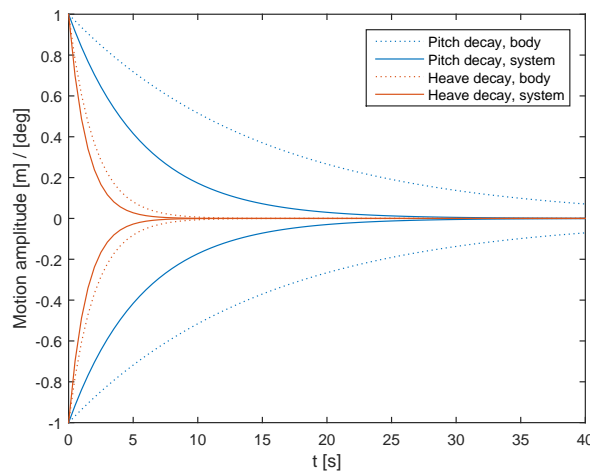
Figure 3.5: Normalized amplitude decay.

From the results it is obvious that the changes to damping is much more evident than the changes in stiffness when going from body- to system-setup. This is to be expected and the behavior of the full system is asserted as acceptable.

3.2   Static Mooring Test

Characterization of the mooring of the OWC WEC is illustrated in the following figures. The characterization was done by a static test, applying a displacement and measuring the resulting load.

Figure 3.6 illustrates the force-displacement curve for a single mooring line, hence the displacement was applied in the direction of the mooring line.
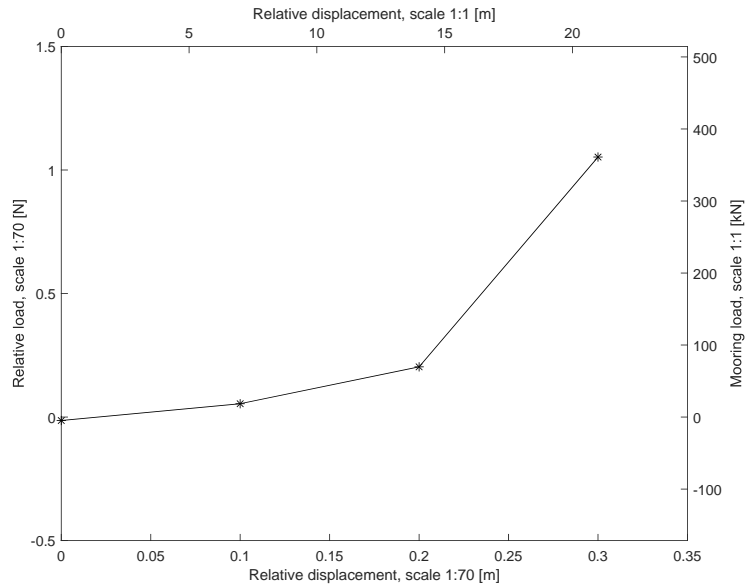

Figure 3.6: Force-displacement curve for single mooring line in scale 1:70 and 1:1.

The force-displacement curve for the total system was determined by applying a displacement in the x-direction (cf. Figure 2.4), measuring the loads in the mooring line and determine the applied load. The following figure illustrates the changes in mooring line loads and the applied horizontal load during the test.
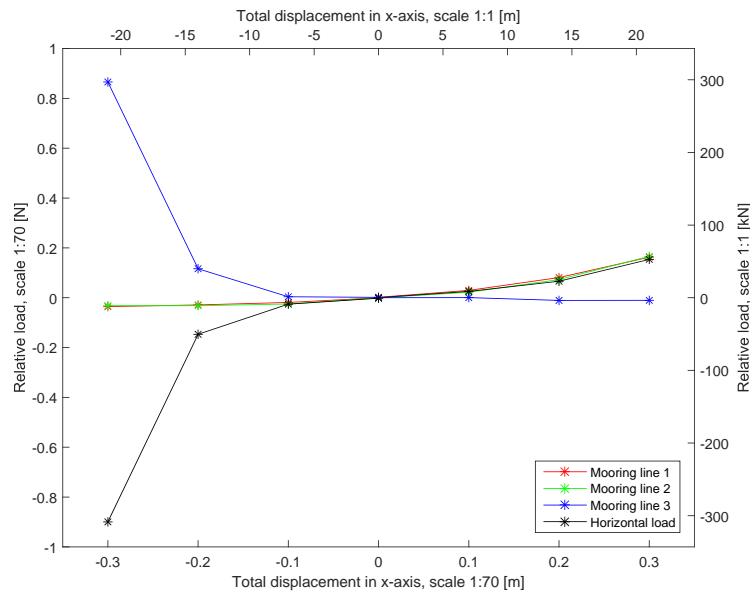
Figure 3.7: Force-displacement curve for total system i the x-direction (cf. Figure 2.4) in scale 1:70 and 1:1.

Finally a displacement was applied in the y-direction, resulting in a curve as illustrated in Figure 3.8.
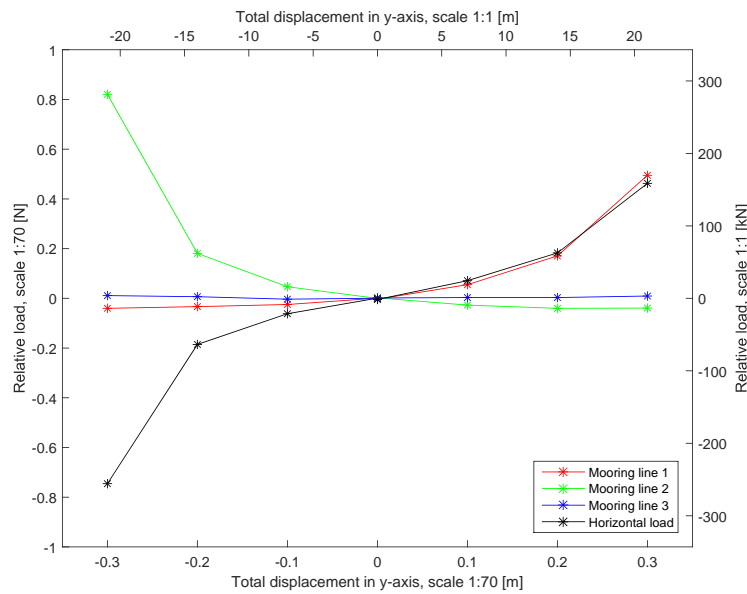

Figure 3.8: Force-displacement curve for total system i the y-direction (cf. Figure 2.4) in scale 1:70 and 1:1.

4 | Wave Details

This chapter serves to highlight the desired and tested sea states and the discrepancies between the two. The quality of the generated waves will be addressed.

4.1 Scatter diagrams

In appendix A a scatter diagram of chosen wave parameters can be seen. The requested waves are defined by H_{m0} and T_E. Since the inputs for the Brestschneider spectrum in the local wave generation software AwaSys 6 (Meinert et al. [2011]) are H_{m0} and T_p, all model scale wave parameters will be presented as such. Note that $T_E = \frac{m_{-1}}{m_0}$ as stated by e.g. Cahill and Lewis [2014].
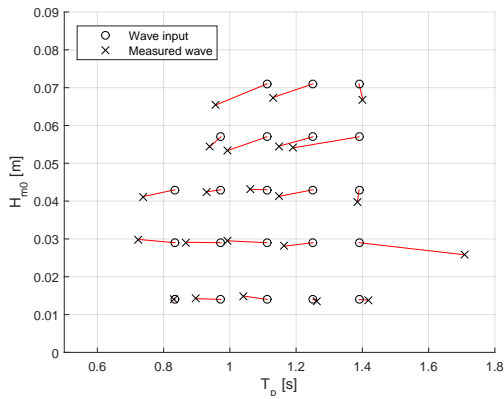
Figure 4.1: Model scale scatter diagram.
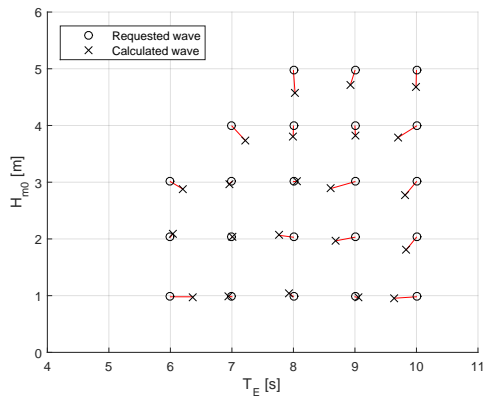
Figure 4.2: Full scale scatter diagram.

4.2 Wave quality

As seen in Figure 4.1 there are some discrepancies between the wave input and the generated wave in the basin. Lower wave height can be due to breaking of

17

the heights waves in the spectrum, lower periods can be caused by cross-modes in the basin and higher periods can be caused by insufficient calm-down time between two runs. As long as only the measured waves are used for analysis, this does not compromise the final results. In Figure 4.2 it is evident that T_E and hence the full scale results are less sensitive to the accuracy of wave periods.
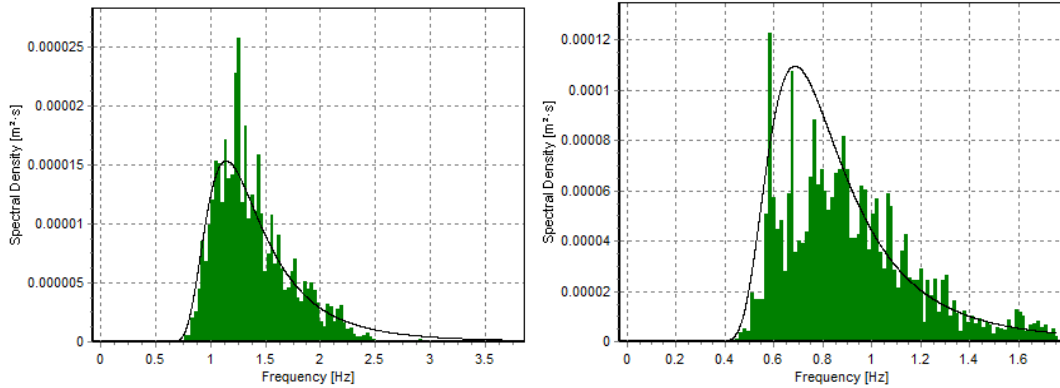

Figure 4.3: Best spectral fit of generated waves.

Figure 4.4: Worst spectral fit of generated waves.

In Figure 4.3 and 4.4 two measured spectra are shown alongside the requested theoretical spectra. The figures represent the best and worst H_{m0}/T_p-fit obtained in the wave basin, cf. Figure 4.1. Best fit is obtained at $H_{m0} = 0.014$ m and $T_p = 0.834$ s, and worst fit at $H_{m0} = 0.029$ m and $T_p = 1.390$ s. All wave conditions have been generated with a duration of 500 waves. This implies that all tests should be able to converge closely to the desired spectral form, but discrepancies can be expected due to reasons stated earlier. The duration necessary to produce 500 waves can be found in appendix A.

5 | Raw Data Time Histories

This chapter aims at illustrating the measurements performed during the test series. Examples of time series will be presented showing power production, mooring loads and motions.

5.1 Power Production

To illustrate the measured pressure difference and the calculated power production, a timeseries for a test with measured wave height and period, $H_{m0} = 0.054$ m and $T_p = 0.938$ s, is shown in Figure 5.1 and a 30 s sample of the test is shown in Figure 5.2.
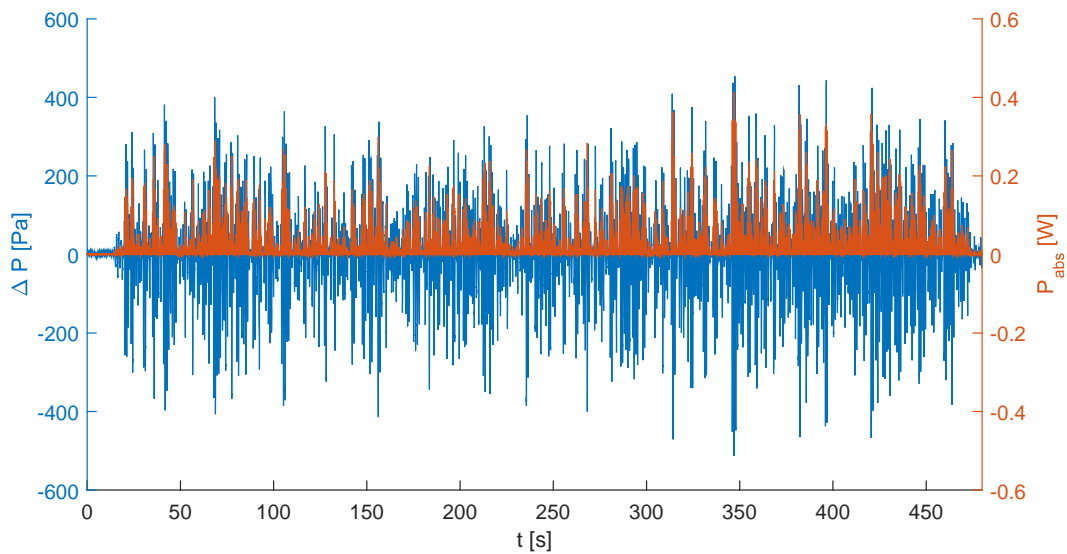

Figure 5.1: Example of time series for power production.

19
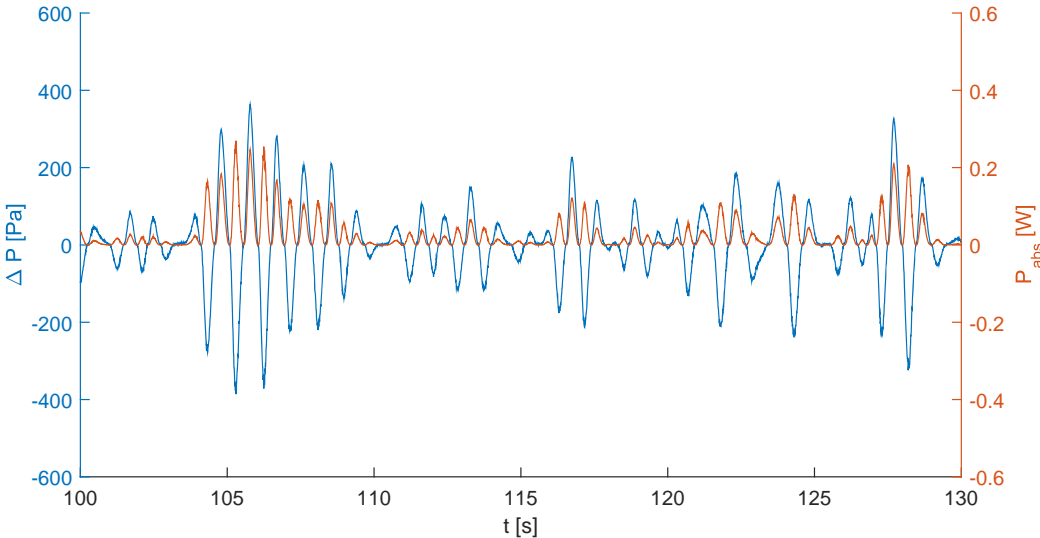
Figure 5.2: Sample of the time series in Figure 5.1

5.2   Mooring Loads

Mooring loads in the three lines were measured throughout all tests. An example of the timeseries from the same test as in the previous section, can be seen in Figure 5.3. In the figure the loads are presented as variations from the initial loads in the test.
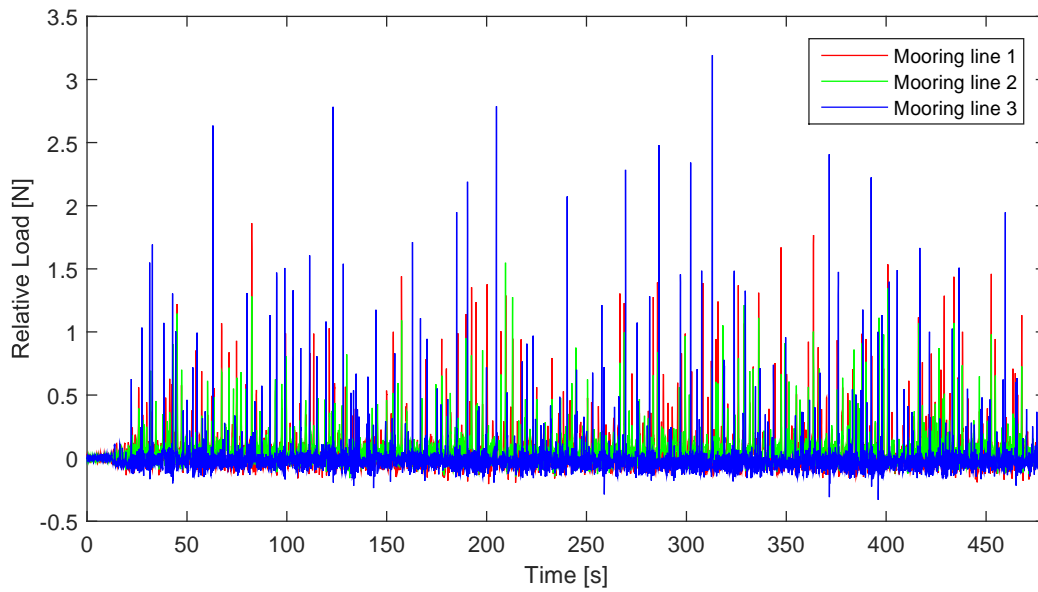
Figure 5.3: Example of mooring load time series.

As seen from the time series, mooring line 3 was exposed to many distinct peak loads, meaning that the highest loads were observed in this line. It was suspected that this was a results of the construction of the buoys, for which reason three additional tests were performed with wave inputs similar to three of the already performed tests, but with a modification of the buoys. An example from the new test with wave input similar to the test in Figure 5.3 can be seen in the following figure. For this test $H_{m0} = 0.056$ m and $T_p = 1.168$ s was measured.
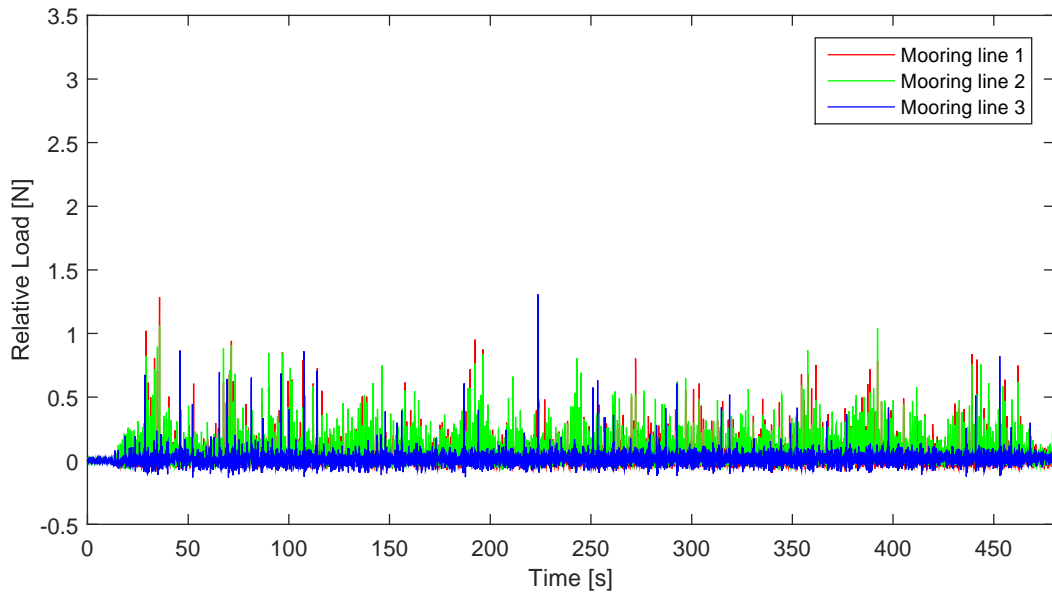
**Figure 5.4:** Example of mooring load timeseries with modified buoys.
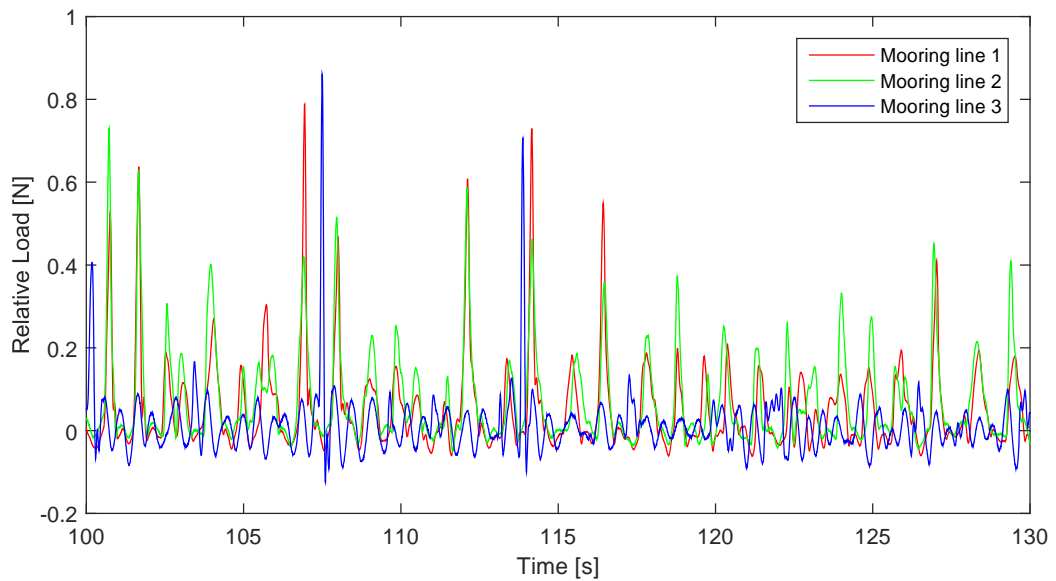
Figure 5.5: Sample of timeseries in Figure 5.4.

The modification of the buoys resulted in much lower loads in mooring line 3 and lower loads in line 1 and 2, which were though not as affected as line 3. Comparing the measured load-surge curve the influence of the modified buoys is clear, cf. Figure 5.6 and 5.7. Most tests were though performed with the

unmodified buoys.
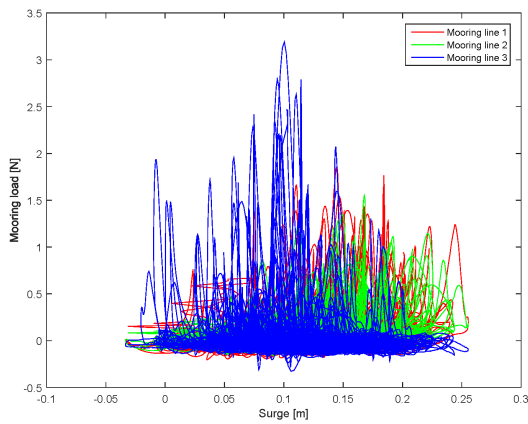
**Figure 5.6:** Example of measured load-surge curve.
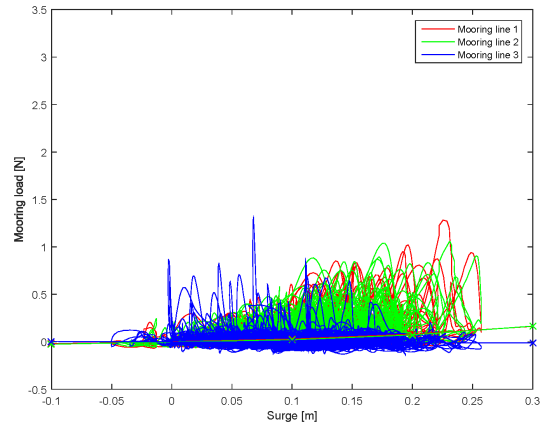
Figure 5.7: Example of measured load-surge curve for a test with modified buoys, together with result from static test.

In figure 5.7 the previously measured static force-displacement curve is shown, illustrating that much higher loads, are observed than in the static tests. This might be a result of the dynamic behaviour of the device under wave attack, and the other motions that it induces. Comparing the load time series with the time series from the motions, a significant correlation is seen. Figure 5.8 illustrates the load together with surge, heave and pitch motions for mooring line 1.
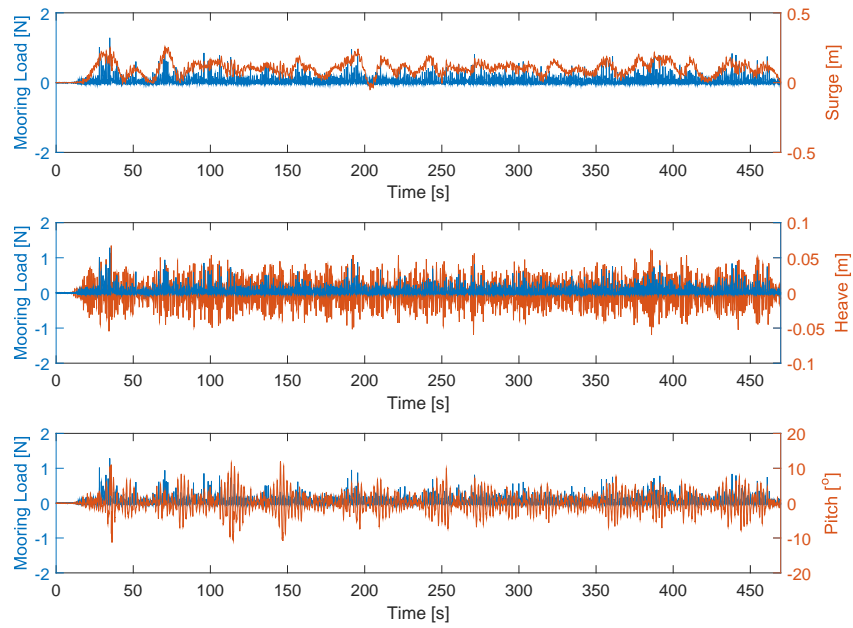
Figure 5.8: Timeseries for the mooring load in line 1 compared to timeseries for measured motions.

By observing the loads and motions in the frequency domain, cf. Figure 5.9 it is clearly seen that the different motions affects the mooring line loads. In chapter 3 the pitch frequency was found to 0.49 Hz and the heave frequency to 1.19 Hz. These corresponds to the frequencies where peaks are observed for the mooring line loads. Similar can be seen for other of the motions.
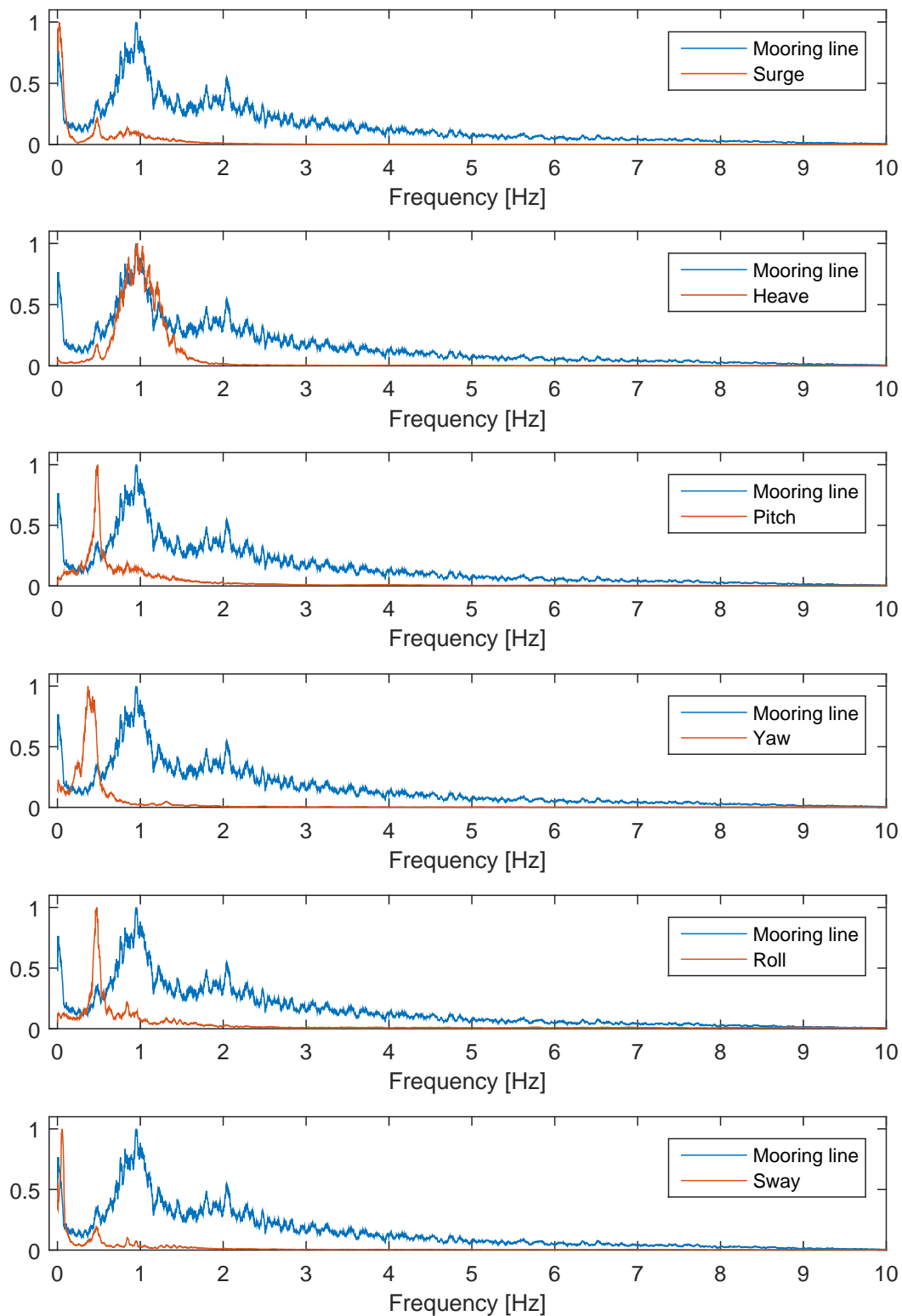
Figure 5.9: Frequency domain analysis of loads and motions. For illustrative purpose each time series is divided with its own maximum value.

6 | Avg. Value Graphs & Charts

This chapter presents the relevant results from the test series as average values of power production and mooring loads. Results are found in both model and full scale values.

6.1 Power Production

The power production is in the following described in terms of the requested full scale scatter diagram and the model scale scatter diagram. The desired data points are marked by ○, but the data user for interpolation is placed at the corrected position marked by ×. The incident wave power, P_W, is obtained from WaveLab 3 by Andersen and Frigaard [2014] and based on the wave celerity. The absorbed power, P_{abs} is calculated as stated in (2.2). Finally the CWR (capture width ratio) is presented for both model and full scale. Note that the CWR does not change in magnitude between the scales since it is a unit-less measure of efficiency, but it is still presented to portrait the efficiency in the same scatter diagram as the other results.

6.1.1 Model Scale

In Figure 6.1 a surface plot of the incident wave power in the conducted tests can be seen. Figure 6.2 shows the measured mean absorbed power.
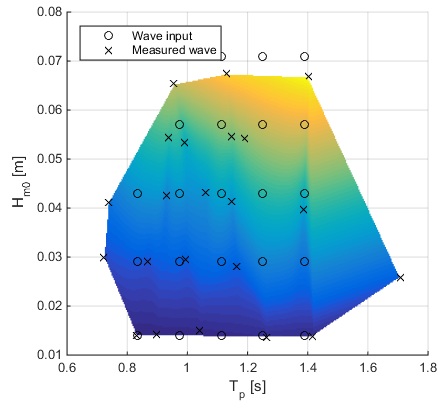
Figure 6.1: Incident wave power in model scale.
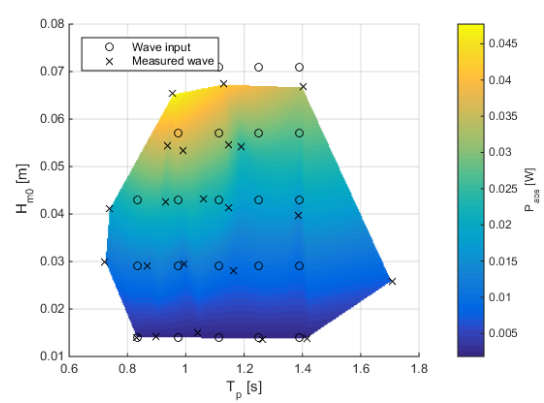
Figure 6.2: Mean absorbed power in model scale.

The CWR presented in Figure 6.3 shows some nonlinearities and a few local maxima and minima, this is due to the attempt of smoothing the surface over data points with varying internal distance.
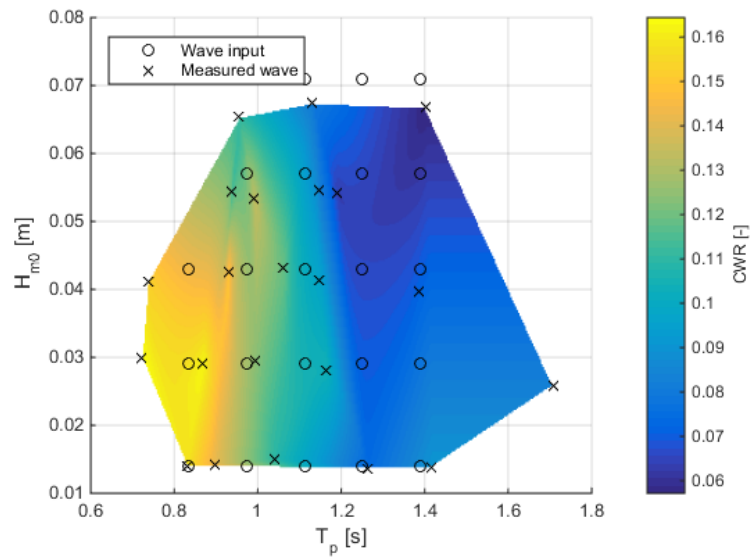

Figure 6.3: CWR in model scale.

6.1.2   Full Scale

Full scale incident wave power is shown in Figure 6.4. The mean absorbed power upscaled to prototype scale can be seen in Figure 6.5.
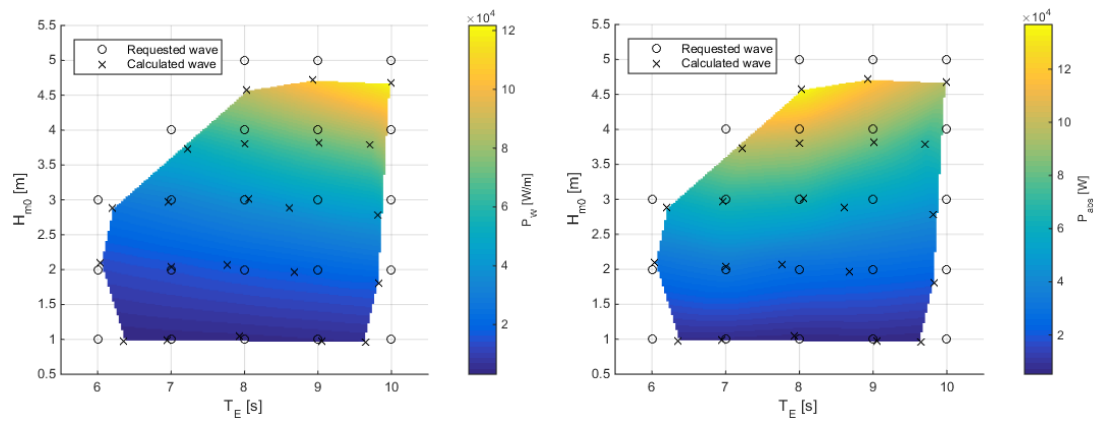
Figure 6.4: Incident wave power in full scale.   **Figure 6.5:** Mean absorbed power in full scale.

In Figure 6.6 the CWR of the full scale system can be seen. The more even distribution of data points results in a smoother representation of the CWR over the area covered by the scatter diagram.
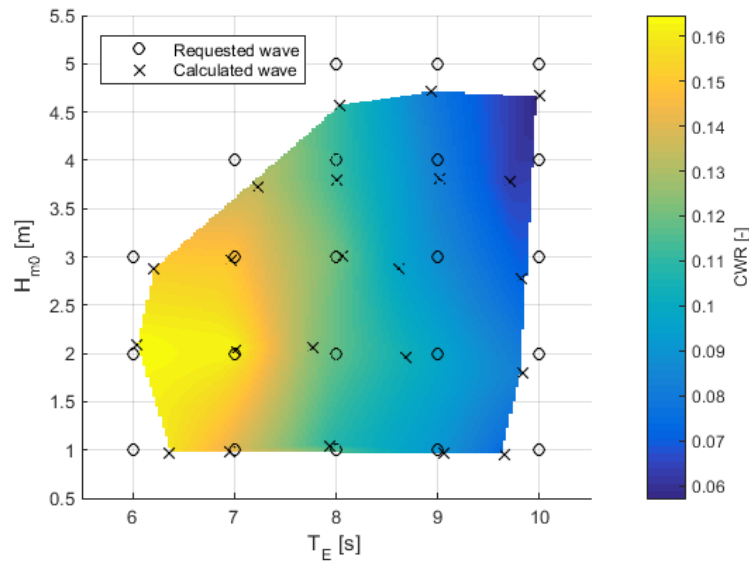

Figure 6.6: CWR in full scale.

6.2 Mooring Loads

Mooring loads are in the following described in the same way as for power production.

The maximum measured mooring loads during tests, when disregarding line 3, are shown in figure 6.7 and 6.8, dependent on the wave height and period.
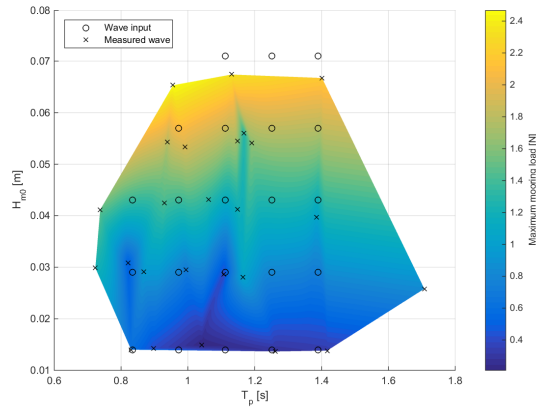
Figure 6.7: Maximum measured load in mooring line 1 and 2.
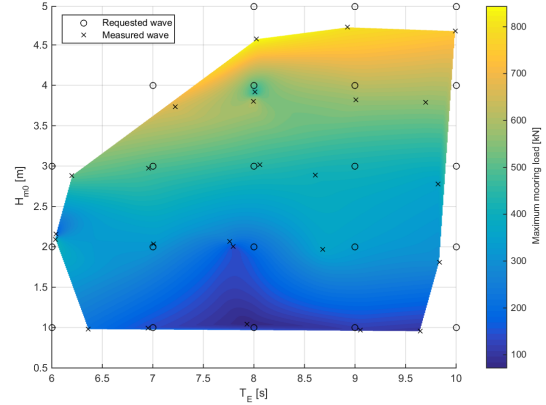
Figure 6.8: Full scale values of maximum mooring load in mooring line 1 and 2.

As seen the mooring loads are highly dependent on the wave height and less dependent on the wave period. Comparing the measured loads in each mooring line (cf. Figure 6.9), the dependency is shown. In the figure maximum loads in mooring line 3 is also stated, showing the much higher peak loads.
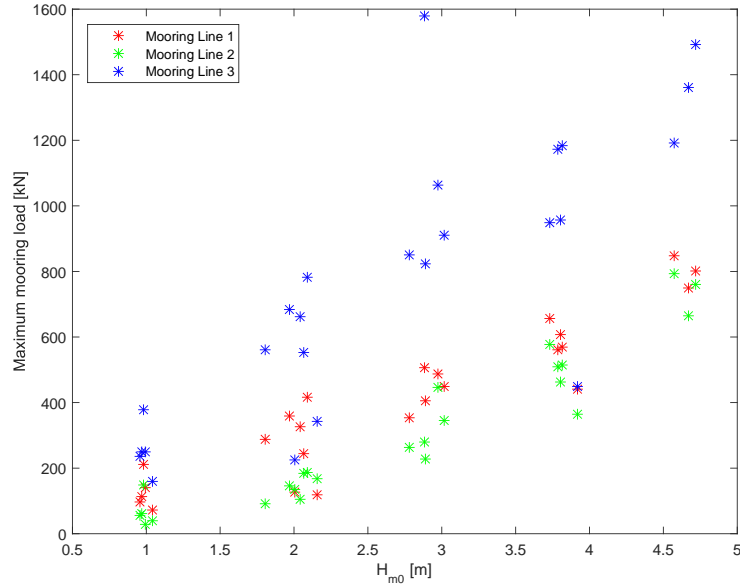

Figure 6.9: Maximum measured mooring loads in the three mooring lines.

7 | Summary Statistics Tables

As some of the surface plots in the prior sections of this technical report can be difficult to read with sufficient precision, this chapter presents some of the key values in tables. All values presented are for the full prototype scale, and hence ready for comparison with the other partners in The Round Robin Programme.

7.1 Wave details

Due to the slight offset of the wave parameters, as presented in chapter 4, the observed wave properties are presented again in Table 7.1 and 7.2. When comparing the production values one should not refer to the wave matrix, but instead take these specific wave details into consideration.

-	-	4.57	4.72	4.67
-	3.73	3.80	3.82	3.79
2.88	2.97	3.02	2.89	2.78
2.09	2.04	2.07	1.97	1.81
0.98	0.99	1.04	0.97	0.95

Table 7.1: H_{m0} [m].

-	-	8.03	8.93	9.99
-	7.22	8.00	9.01	9.70
6.20	6.96	8.06	8.61	9.82
6.03	7.01	7.76	8.68	9.83
6.36	6.95	7.93	9.05	9.64

Table 7.2: T_E [s].

7.2 Power production

One of the key comparison points of The Round Robin Programme is expected to be the power production. The mean effect of the system in prototype scale is previously presented as a surface in Figure 6.5. In Table 7.3 the values used for the interpolated surface can be seen.

Due to the uncertainties in the discharge coefficient, c_d, used for the calculation of the power production in (2.2) and (2.3) the true production might vary significantly. The theoretical limits of 0.62-0.88 are presented in section

-	-	137.3	121.3	97.3
-	96.9	97.0	83.0	68.6
55.3	66.2	64.9	52.5	42.3
30.5	34.1	30.4	26.4	20.6
6.8	6.9	7.0	5.8	5.0

Table 7.3: Estimated effect of WEC [MW].

2.4. When this lower and upper limit is applied, the range of production effect is as shown in Table 7.4.

|				
-	-	133-189	118-167	94-134
-	94-133	94-133	80-114	66-94
54-76	64-91	63-89	51-72	41-58
30-42	33-47	29-42	26-36	20-28
7-9	7-10	7-10	6-8	5-7

Table 7.4: Theoretical ranges of effect for WEC [MW].

Bibliography

Andersen, T. L. and Frigaard, P. (2014). *WaveLab 3.*

Cahill, B. and Lewis, T. (2014). Wave period ratios and the calculation of wave power. In *Proceedings of the 2nd Marine Energy Technology Symposium, METS2014.*

Joachim, W. (1926). *An Investigation of the Coefficient of Discharge of Liquids through Small Round Orifices.* National Advisory Committee for Aeronautics.

Meinert, P., Andersen, T. L., and Frigaard, P. (2011). *AwaSys 6 User Manual.*

Nielsen, K., Jacobsen, F. P., Simonsen, M., and Scheijgrond, P. (2013). *Attenuator development phase I.* Infrastructure Access Report: KNSWING. Marinet.

A | Definition of Wave States

This appendix includes a brief overview of desired sea states and the actual parameters used for inputs in the laboratory tests.

0,0143   0,1195

Full scale   Requested

H_m0							
5							
4							
3							
2							
1							
	4	5	6	7	8	9	10 T_E

Model 1:70   Requested

H_m0							
0,071							
0,057							
0,043							
0,029							
0,014							
	0,4781	0,5976	0,7171	0,8367	0,9562	1,0757	1,1952 T_E

Model 1:70   To be run

H_m0								Drop:
0,071	501	502	503	504	505	506	507	Under 0.8s Tp
0,057	401	402	403	404	405 415	406	407	Steepness > 4%
0,043	301	302	303	304	305	306	307	
0,029	201	202	203 213	204	205 215	206	207	
0,014	101	102	103	104	105	106	107	
	0,556	0,695	0,834	0,973	1,112	1,251	1,390 T_p	

#waves	500	277,96	347,45	416,94	486,43	555,92	625,41	694,9	sec
startup	0	4,6327	5,7908	6,949	8,1072	9,2653	10,424	11,582	min

B | List of Executed Tests

On the following pages an overview of executed tests can be found.

Test #	H_m0 [m]	T_p [s]	Wavelab File name	Optitrack File name	Comment	Done
101	0.014	0.556	-	-	Omitted: Basin period limit	X
102	0.014	0.695	-	-	Omitted: Basin period limit	X
103	0.014	0.834	103	103	OptiTrack time-error	X
104	0.014	0.973	104	104		X
105	0.014	1.112	105	105		X
106	0.014	1.251	106	106		X
107	0.014	1.390	107	107		X
201	0.029	0.556	-	-	Omitted: Steepness > 4%	X
202	0.029	0.695	-	-	Omitted: Basin period limit	X
203	0.029	0.834	203	203	OptiTrack time-error	X
204	0.029	0.973	204	204		X
205	0.029	1.112	205	205		X
206	0.029	1.251	206	206		X
207	0.029	1.390	207	207		X
213	0.029	0.834	213	213		X
215	0.029	1.112	215	215		X
301	0.043	0.556	-	-	Omitted: Steepness > 4%	X
302	0.043	0.695	-	-	Omitted: Steepness > 4%	X
303	0.043	0.834	303	303	OptiTrack time-error	X
304	0.043	0.973	304	304		X
305	0.043	1.112	305	305		X
306	0.043	1.251	306	306		X
307	0.043	1.390	307	307		X
401	0.057	0.556	-	-	Omitted: Steepness > 4%	X
402	0.057	0.695	-	-	Omitted: Steepness > 4%	X
403	0.057	0.834	-	-	Omitted: Steepness > 4%	X
404	0.057	0.973	404	404	h=0.9	X
405	0.057	1.112	405	405		X
406	0.057	1.251	406	406		X
407	0.057	1.390	407	407		X
415	0.057	1.112	415	415		
501	0.071	0.556	-	-	Omitted: Steepness > 4%	X
502	0.071	0.695	-	-	Omitted: Steepness > 4%	X
503	0.071	0.834	-	-	Omitted: Steepness > 4%	X
504	0.071	0.973	-	-	Omitted: Steepness > 4%	X
505	0.071	1.112	505	505		X
506	0.071	1.251	506	506		X
507	0.071	1.390	507	507		X
901	-	-	901	-	Load cell 1 2 3 calibration. 0g 100g 500g 1000g	X
902	-	-	902	-	Anchor system. 1,2,3,+X,-Y,+Y [0,10,20,30,20,10,0]	X
903	-	-	903	-	System mean test	X
904	-	-	904	-	Load cell 1 re-calibration. 0g 100g 500g 1000g	X
905	0.02	1.4	905	-	Test of mooring response	X
911	-	-	-	911	Heave decay, unmoored, no tube	X

912	-	-	-	912	Pitch decay, unmoored, no tube	X
913	-	-	-	913	Heave deacy, moored, no tube	X
914	-	-	-	914	Heave decay, moored, tube	X
915	-	-	-	915	Pitch decay, moored, tube	X
920	-	-	-	920	Surge,sway,heave,roll,pitch,yaw	X
921	-	-	-	921	Heave decay, unmoored, no tube	X
922	-	-	-	922	Pitch decay, unmoored, no tube	X
923	-	-	-	923	Heave deacy, moored, no tube	X
924	-	-	-	924	Heave decay, moored, tube	X
925	-	-	-	925	Pitch decay, moored, tube	X